

# ANALYTICAL FORMULATION OF THE FRACTURE PATH AND SHEAR RESISTANCE FOR RC BEAMS

Luis Saucedo\*, Rena C. Yu<sup>†</sup> and Gonzalo Ruiz<sup>†</sup>

\* University of Oxford  
Department of Materials, Parks Road, OX1 3PH Oxford, UK

<sup>†</sup>University of Castilla-La Mancha  
Avda. Camilo José Cela s/n, 13071 Ciudad Real, Spain

**Key words:** Shear resistance, cohesive model, fracture process zone,

**Abstract.** Shear design for reinforced concrete beams is of significant technological interest. Numerous experimental and numerical work have been developed to predict the shear resistance of reinforced beams. In this work, we consider the fracture path as the equilibrium trajectory resulted from external loads and internal forces; assuming a linear-decreasing cohesive law for concrete bulk, fully-developed fracture process zone size as a material parameter, a perfect plastic bond-slip relation for the interface between steel rebar and concrete, analytical predictions for the crack path and shear resistance for beams with arbitrary geometry, longitudinal and/or shear reinforcement ratio, are derived and validated against available experimental data, the agreement is remarkable.

## 1 INTRODUCTION

Shear design in reinforced concrete structures is of significant technological interest, as a result, numerous models have been developed to estimate the shear resistance of reinforced beams, for an incomplete list, see [1, 2, 3, 4, 5, 6, 7, 8, 12, 9, 22] and the references within. Among these models, the first widely-applied is the Modified Compression Field Theory (MCFT) developed by Vecchio and coworkers [2, 4, 8, 12, 22], which is actually a smeared rotating crack model with compression softening and tension stiffening. The size effect model by Bazant and Kim [1], starting from a predetermined fracture path, neglecting multiple tensile cracks and the dowel action of reinforcements, was applied to diagonal tension failure of longitudinally reinforced concrete beams; some years later Karihaloo [7] extended it to beams with stirrups. Along this line, the two-parameter fracture model by Jenq and Shah [6]

assumes a diagonal-tension failure and takes Mode-I fracture toughness as the crack growth criterion. The third group is based on the fictitious crack approach by Gustasson and Hillerborg [5].

In this work, we assume the concrete bulk as an elastic material until cracking, the tensile strength as the crack initiation and propagation criterion, the concrete fracture is governed by a linear-decreasing cohesive law. In this way, multiple potential cracks are considered naturally, the propagation or arrest of each individual crack as external load increases can also be predicted.

The rest of this paper is structured as follows. The layout of the physical problem is explained in Section 2. The fracture path and shear resistance are calculated analytically and validated in Section 3. Finally, relevant conclusions are drawn in Section 4.

## 2 ANALYTICAL FORMULATION OF A COHESIVE CRACK PROPAGATION IN A BEAM WITH REINFORCEMENTS

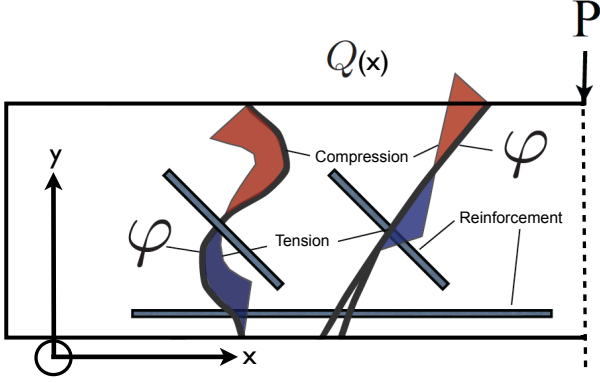


Figure 1: Possible stress distribution along distinct fracture path and the function that defines each potential crack  $x = \phi(y)$ .

Consider a beam of rectangular section with longitudinal and inclined reinforcements, all possible crack trajectories described by a series of functionals  $x = \phi(y)$  can be determined from the equilibrium states, see Fig. 1. Thus the inclination angle  $\alpha$  of the crack path defined by

the non-dimensional function  $x^* = \phi(y^*)$  with respect to the x-axis can be calculated accordingly

$$\sin \alpha = \frac{1}{\sqrt{\phi'(y^*)^2 + 1}} \quad (1)$$

$$\cos \alpha = \frac{\phi'(y^*)}{\sqrt{\phi'(y^*)^2 + 1}} \quad (2)$$

where we have normalized all length variables by the beam depth  $H$ , i.e.  $x^* \in [0, \eta]$ ,  $y^* \in [0, 1]$ . Through equilibrium conditions, the flexural moments with respect to the neutral axis, the shear forces in the vertical direction and self-balance between compressive and tensile forces in the horizontal direction can be written as follows

$$M_i = M_c + M_t \quad (3)$$

$$Q_y = F_{c_y} + F_{t_y} \quad (4)$$

$$F_{c_x} = F_{t_x} \quad (5)$$

The compressive and tensile forces and their non-dimensional counterparts are calculated as follows

$$F_c = \sigma_c \frac{y - y_n}{H - y_n} \frac{1}{\sin \alpha} \quad (6)$$

$$F_t = \left( \frac{y_n - y}{y_n - y_{ud}} + \frac{y - y_{tip}}{y_{ud} - y_{tip}} \right) \frac{1}{\sin \alpha} \quad (7)$$

$$F_c^* = \frac{F_c}{f_t B H} = \sigma_c^* \frac{y^* - y_n^*}{1 - y_n^*} \sqrt{\phi'(y^*)^2 + 1} \quad (8)$$

$$F_t^* = \frac{F_t}{f_t B H} = \sqrt{\phi'(y^*)^2 + 1} \left( \frac{y_n^* - y^*}{y_n^* - y_{ud}^*} + \frac{y^* - y_{tip}^*}{y_{ud}^* - y_{tip}^*} \right) \quad (9)$$

Where  $y_n$ ,  $y_{ud}$  and  $y_{tip}$  are the vertical coordinates of the neutral axis, the undamaged material (end of the FPZ, or the cohesive crack tip) and the tip of the stress-free crack respectively.

Replacing in Eqn. 4, we get the equilibrium equation:

$$\begin{aligned}
 Q^*(x_0) = \frac{Q(x_0)}{f_t B H} &= \int_{y_n^*}^1 \frac{y^* - y_n^*}{1 - y_n^*} \sigma_c^* \varphi'(y^*) dy^* + \int_{y_{ud}^*}^{y_n^*} \frac{y_n^* - y_d^*}{y_n^* - y^*} \varphi'(y^*) dy^* \\
 &+ \int_{y_{tip}^*}^{y_{ud}^*} \frac{y^* - y_{tip}^*}{y_{ud}^* - y_{tip}^*} \varphi'(y^*) dy^* + f_y^* \rho_i \sin \theta
 \end{aligned} \quad (10)$$

From the compatibility of stresses we get

$$\sigma_c^* = \frac{\sigma_c}{f_t} = \frac{1 - y_n^*}{y_n^* - y_{tip}^* - 1/\beta} \quad (11)$$

## 2.1 Fracture trajectory

Consider  $\varphi$  as a known function, plug  $y_n^*$  and  $\sigma_c^*$  into Eqn. 10, we can solve to get the function  $\varphi$  as follows

$$\varphi(y^*) = a_1 (a_2 y^{*3} + a_3 y^{*2} + a_4 y^*) + a_5 \quad (12)$$

We impose two limit conditions to determine the five coefficients  $a_1$  to  $a_5$ , one is when the longitudinal reinforcement ratio tends to infinity, the fracture tends to the minimum shear point, the other is when the longitudinal and inclined ratios tends to zero, the fracture tends to

the plain concrete fracture previously known.

$$a_5 = \frac{x_0^*}{\eta} = \frac{x_0}{\eta H} \quad (13)$$

$$a_4 = 2\beta\beta_1 f_c^* \frac{Q^*(x_0) - \sigma_{ir}^*}{1 + 2\sigma_{lr}^* + \sigma_{ir}^*} \quad (14)$$

$$a_3 = \frac{1 + 2\sigma_{lr}^{*3} + \sigma_{ir}^{*3}}{24} a_4 \quad (15)$$

$$a_2 = \frac{2}{3(1 + \sigma_{ir}^{*2})} a_3 \quad (16)$$

$$a_1 = \frac{x_{null}^* - x_0^*}{a_2 \gamma^3 + a_3 \gamma^2 + a_4 \gamma} \quad (17)$$

$$\gamma = 1 + \frac{f_t B (1 + \sigma_{ir}^*)}{f_c^* q} e^{-\sigma_{lr}^*} \quad (18)$$

$$\sigma_{lr}^* = \rho_l f_y^* \quad (19)$$

$$\sigma_{ir}^* = 0.75 \rho_i f_y^* \sin \theta \quad (20)$$

where  $q$  is the distributed load per unit of length,  $x_{null}^*$  in a three point bending test is 0.5,  $\sigma_{lr}^*$  and  $\sigma_{ir}^*$  are the normalized average stress of the longitudinal and inclined reinforcements Eqn. 19, and  $\sigma_{ir}^*$  respectively. The angle  $\theta$  is that of the inclined reinforcement, defined as  $45^\circ$ .

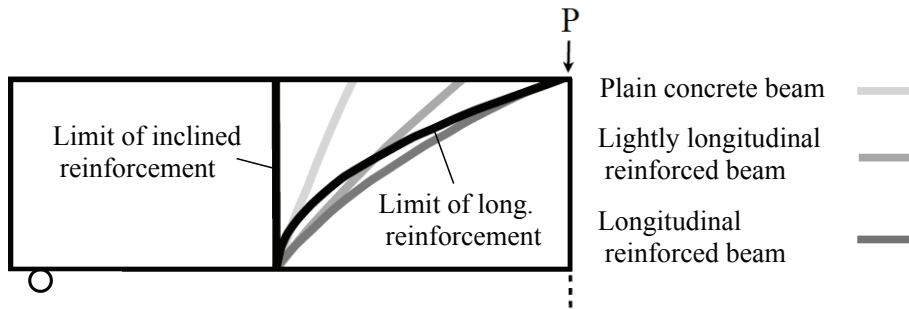


**Figure 2:** Sensitivity of the reinforcement ratio on the crack path initiated at a quarter span from the support.

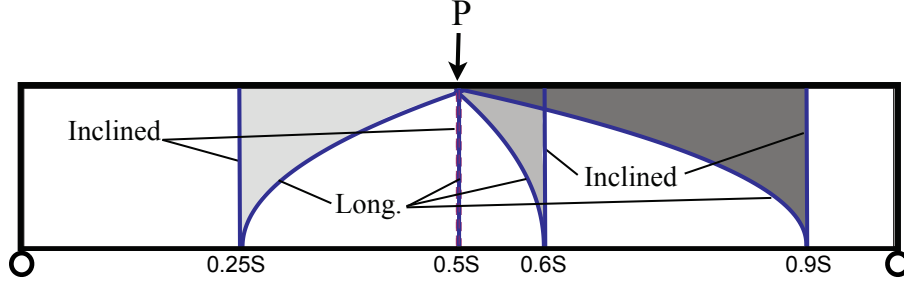


**Figure 3:** Limit curves of the fracture path initiated from several locations when there is zero or infinite reinforcements.

It needs to be pointed out that, in the limit case of heavy longitudinal or inclined reinforcement, the function  $\varphi$  can be significantly simplified. For example, the limit curve for longitudinal reinforcement could be described by the Eqn. 12 with the coefficients  $a_{1l}$  to  $a_{5l}$ . Those limit curves are plotted in Fig. 3.

$$a_{5l} = \frac{x_0^*}{\eta} = \frac{x_0}{\eta H} \quad (21)$$

$$a_{4l} = 2\beta\beta_1 \frac{f_c^* Q^*(x_0)}{1 + 2T_0^*} \quad (22)$$

$$a_{3l} = a_{4l} \left( \frac{1}{24} + \frac{1}{12} T_0^{*3} \right) \quad (23)$$

$$a_{2l} = \frac{2}{3} a_{3l} \quad (24)$$

$$a_{1l} = \frac{x_{null}^* - x_0^*}{a_{2l} + a_{3l} + a_{4l}} \quad (25)$$

where  $T_0$ , which is the reinforcement strength  $\rho_l f_y$ , fitted as 10 MPa, sets the limit curve

## 2.2 The external load that corresponds to each possible crack trajectory

Once the trajectory of crack initiated from a position  $x_0$  is define by Eqn. 12, we can ana-

- Moment generated by the compressive tractions

$$M_c^* = \frac{M_c}{BH^2 f_t} = \frac{1}{2} \sigma_c^* \sqrt{(y_n^* - y_{cgc}^*)^2 + (x_n^* - x_{cgc}^*)^2} \sqrt{(1 - y_n^*)^2 + (x_h^* - x_n^*)^2} \quad (26)$$

where  $y_{cgc}^* = y_n^* + \frac{2}{3}(1 - y_n^*)$ ,  $x_{cgc}^* = \varphi(y_{cgc}^*)$ ,  $x_h^* = \varphi(1)$  and  $x_n^* = \varphi(y_n^*)$

- Moment generated by the tensile tractions

$$M_t^* = \frac{M_t}{BH^2 f_t} = \frac{1}{2} \sqrt{(y_n^* - y_{cgt}^*)^2 + (x_n^* - x_{cgt}^*)^2} \sqrt{(y_n^* - y_{tip}^*)^2 + (x_n^* - x_{tip}^*)^2} \quad (27)$$

for strongly reinforced beams, beyond which, the crack trajectory will coincide with the limit curve as shown in Fig. 3.

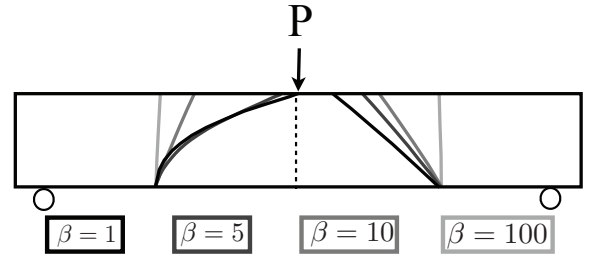


**Figure 4:** Sensitivity of the parameter  $\beta$  for reinforced (left) and plain (right) concrete beams.

The sensitivity of the parameter  $\beta$  on the trajectory of a crack initiated from a quarter span to either of the support for a reinforced or plain concrete beam is shown in Fig. 4. Note that when  $\beta$  increases, the crack tends to move away from the loading point.

lytically obtain the corresponding external load through equilibrium considerations. The flexural moment generated by compressive or tensile forces and the longitudinally rebars are illustrated in the following equations.

where  $y_{cgt}^* = \frac{1}{2}(y_n^* - y_{tip}^*)$ ,  $x_{cgt}^* = \varphi(y_{cgt}^*)$ ,  $x_{tip}^* = \varphi(y_{tip}^*)$  and  $x_n^* = \varphi(y_n^*)$

- Moment generated by the longitudinal rebars

$$M_{lr}^* = \frac{M_{lr}}{f_t B H^2} = \rho_l f_y^* (y_n^* - c^*) \exp[-\varphi'(y_{tip}^*)] \quad (28)$$

where  $c^*$  is the normalized cover length. The moment given by the inclined reinforcement can also be easily calculated the same way.

- Internal moment

$$M_i^* = M_{lr}^* + M_t^* + M_c^* \quad (29)$$

For the case of a three point bending configuration, the external load  $P$  is related with the internal moment as follows:

$$P^* = \frac{P}{f_t B H} = \frac{2M_i^*}{x_0^*} \quad (30)$$

The above expression, Eqn. 30, slightly modified, can be extended to any load distribution on the top surface. Therefore, we have analytically determined the load capacity for a beam with arbitrary load, reinforcement ratio or span-depth ratio. For the purpose of clarification, we classify the concrete beams into three categories, those slightly reinforced with longitudinal rebars, those heavily reinforced with longitudinal rebars and those have both longitudinal and inclined rebars.

### Beams lightly reinforced with longitudinal bars

We consider a beam is lightly reinforced when the reinforcement rate is lower than  $T_0$ . The technological application of this kind of beams is the prevention of brittle failure. In this case, the compressive stress at the top of the beam has not reached the compressive strength, and its value is determined through equilibrium equations. By comparing the failure load for various trajectories initiated from different locations of the beam, the minimum failure load is given by the trajectory started at the position  $S/4$ , the ultimate shear force is given by Eq. 31.

$$V_u^* = \frac{V_u}{B H f_t} = \frac{d_{cy}^*}{3\eta} \frac{\sigma_c^{*2}}{\sigma_c^* + 1} + \sigma_y^* \rho_l \frac{1 - c^*}{\eta} \quad (31)$$

$$d_{cy}^* = \left(1 - \frac{1}{2\beta}\right)$$

$$\sigma_c^* = f_y^* \rho_l + \sqrt{1 + \frac{4d_{cy}^*}{f_y^* \rho_l}} \quad (32)$$

where  $c^*$  is the normalized covering length  $c/H$ . Note that the parameters such as  $\eta$ ,  $\beta$  y  $l_{fpz}$  all play a role in the failure load.

### Beams strongly reinforced with longitudinal bars

In contrast, a beam is considered as strongly reinforced when the reinforcement rate is higher than  $T_0$ . In this case, the compressive stress at the top of the beam attains the strength  $f_c$ . The shear force for failure is obtained as follows

$$V_u^* = \frac{V_u}{f_t B H} = \frac{1}{2} \frac{P_I}{f_t B H} + (1 + f_c^*) d_{cy}^{*2} \frac{\tan^2 \alpha}{2\eta} \quad (33)$$

where

$$d_{cy}^* = \left(1 - \frac{1}{2\beta}\right) \quad (34)$$

$$\alpha = \alpha_0 \ln \eta \quad (35)$$

where  $\alpha_0 = 25.35$ , and  $P_I$  is the peak load for a Mode-I failure of the same beam under three-point-bend load configuration. Note that

the first term in Eq. 33 is influenced by material properties, geometry and reinforcement ratio, whereas the second term is only influenced by the material properties and the geometry, not the reinforcement ratio.

### Beams reinforced with longitudinal and inclined bars.

In this case, the beams are reinforced with both kind of reinforcements, the corresponding shear force of failure is written as follows:

$$V_u^* = \frac{V_u}{f_t B H} = \frac{f_c^* d_{cy}^2 \tan^2 \alpha}{3\eta - 6d_{cy}^* \tan \alpha} \quad (36)$$

$$d_{cy}^* = \left(1 - \frac{1}{2\beta}\right)$$

$$\alpha = \left[ \alpha_0 + \left( \frac{c_0^* f_y^* \rho_l \rho_i}{\eta} - 1 \right) \right] \ln \eta \quad (37)$$

where  $c_0^* = \frac{0.0003 f_t^2}{0.08 f_c^{0.5}}$  and  $\alpha_0 = 25.35^\circ$ . Part of the term  $c_0$  is minimum shear reinforcement for a beam according with the Euro Code 2.

## 3 VALIDATION AND TECHNOLOGICAL APPLICATION

In this Section, we first validate the predicted crack path against the experimental ones given by Carpinteri et al. [17]. Then we compare the failure load obtained from Eqns. 33, 31 and 36 to that given by the Euro Code 2 [20] and the Model Code.

### 3.1 Validation of the crack path

In order to verify the ability of Eq. 12, we compare various crack trajectories initiated at different locations of the beam with the experimentally observed ones by Carpinteri et al. [17]. The material properties and beams dimensions are given in Tab. 1. The beams were reinforced with rebars of diameter of 8, 12 and 20 mm respectively, the resulted reinforcement ratios are of 0.25% ( $1\phi 8$ ), 0.50% ( $2\phi 8$ ), 1.12% ( $2\phi 12$ ) or 3.14% ( $2\phi 20$ ).

Table 1: Material properties and beam geometry for the concrete tested by Carpinteri et al. [17].

E [GPa]	$f_c$ [MPa]	$f_t$ [MPa]	$G_F$ [N/m]
33.1	49.4	4.2	111.5
$l_{fpz}$ [mm]	B [mm]	H [mm]	S [mm]
18	200	100	1200

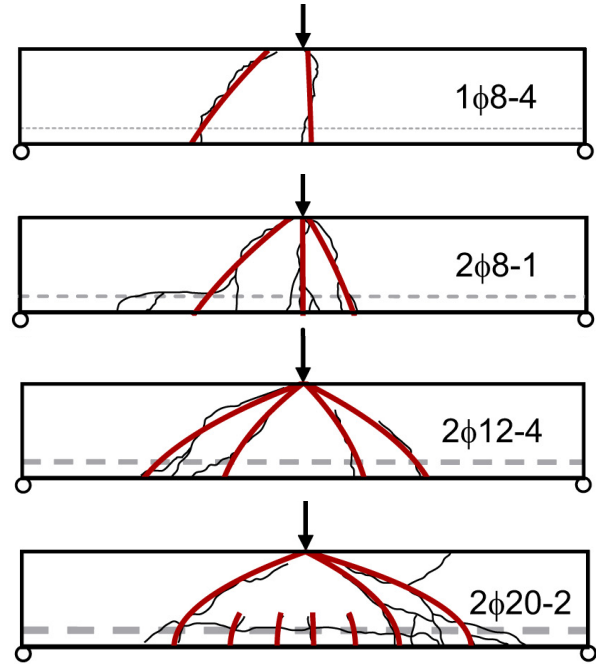


Figure 5: Predicted and observed crack trajectories by Carpinteri et al. [17] for beams with the same geometry and different longitudinal reinforcement ratios.

### 3.2 Validation of the load capacity

In this section, we validate our analytical model against experimental results for the load capacity of beams lightly or strongly reinforced with longitudinal rebars, or beams with both longitudinal and inclined rebars. The material properties and beam dimensions as well as reinforcement ratios for different beams are shown in Tabs. 2-4 respectively.

**Table 2:** Experimental results of Mathey et al. [29] for lightly longitudinal reinforced concrete beams.

Test No.	$\eta$	H [mm]	B [mm]	$f_c$ [MPa]	$f_y$ [MPa]	$\rho_l$ [%]
1	1.29	403	203	24	500	0.75
2	1.29	403	203	26	500	0.75
3	1.29	403	203	27	500	0.75
4	1.29	403	203	26	500	0.75
5	1.29	403	203	27	500	1.16
6	1.29	403	203	26	500	1.16
7	1.29	403	203	23	500	1.17
8	1.29	403	203	23	500	1.17

**Table 3:** Experimental results of Moody et al [30] for strongly longitudinal reinforced concrete beams.

Test No.	$\eta$	H [mm]	B [mm]	$f_c$ [MPa]	$f_y$ [MPa]	$\rho_l$
1	1.14	553	178	18	500	2.72
2	1.14	553	178	21	500	2.72
3	1.14	553	178	22	500	2.72
4	1.14	553	178	23	500	2.72
5	1.14	553	178	18	500	3.46
6	1.14	553	178	23	500	3.46
7	1.14	553	178	24	500	3.46
8	1.14	553	178	25	500	3.46
9	1.14	553	178	21	500	4.25
10	1.14	553	178	22	500	4.25
11	1.14	553	178	22	500	4.25
12	1.14	553	178	25	500	4.25

**Table 4:** Experimental results of Kazemi et al [21] for longitudinal and inclined reinforced concrete beams

Test No.	$\eta$	H [mm]	B [mm]	$f_c$ [MPa]	$f_y$ [MPa]	$\rho_l$ [%]	$\rho_i/\rho_{min}$
1	4.85	330	200	38.3	225	1.68	2.0
2	4.64	345	200	38.3	225	1.07	2.0
3	4.44	360	200	38.3	922	0.18	8.1
4	4.64	345	200	38.3	922	0.26	8.1
5	4.80	333	200	38.3	922	0.34	8.1
6	4.76	336	200	38.3	922	0.35	8.1
7	4.85	330	200	38.3	922	0.41	8.1

The comparison are illustrated in Figs. 6-8 for those beams tested by Mathey et al. [29], Moody et al [30] and Kazemi et al. [21] respectively. It is noteworthy that, our analytical model gives a better prediction than the Euro Code 2 and Model Code for all the examples demonstrated.

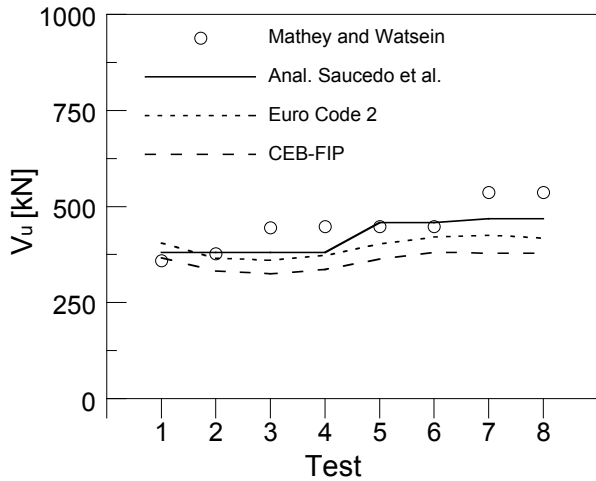


Figure 6: Prediction for lightly reinforced beams with longitudinal rebars tested by Mathey et al. [29].

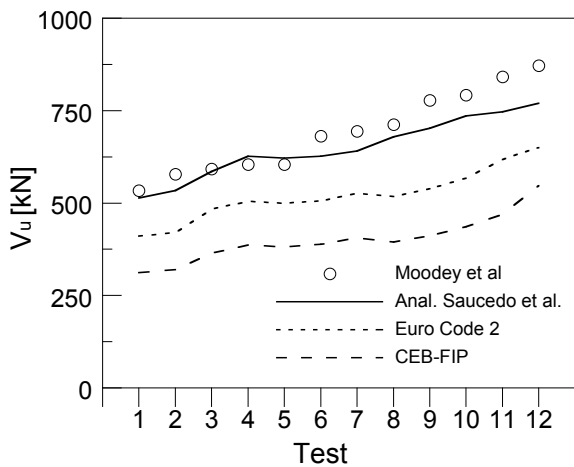


Figure 7: Prediction for strongly reinforced beams with longitudinal rebars tested by Moody et al. [30].

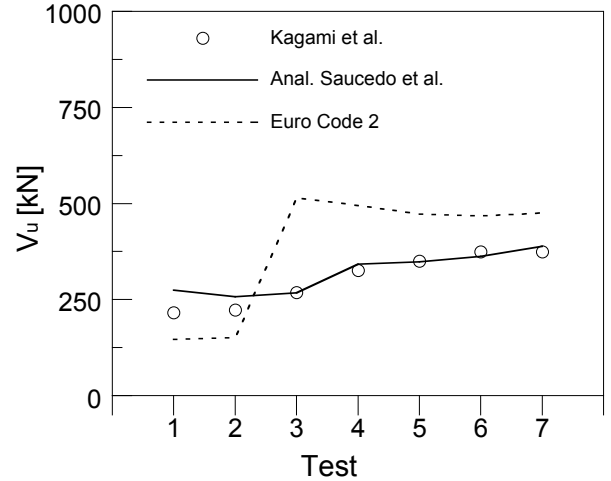


Figure 8: Prediction for beams with both longitudinal and inclined rebars, tested by Kazemi et al. [21].

## 4 CONCLUSIONS

Assuming a linear-decreasing cohesive law for concrete fracture, a perfect bond-slip relation for the steel-concrete interface, we have developed an analytical method to predict the shear resistance for a beam reinforced with any ratio of longitudinal and transversal rebars. The formulation has been validated against numerous experimental results for fracture path and ultimate loads. The agreement is remarkable.

## NOMENCLATURE

- $f_t$ ,  $f_c$  and  $G_F$ : Concrete tensile, compressive strength and specific fracture energy.
- $w_c$ : Critical opening displacement in a locally mode-I cohesive crack.
- $l_{fpz}$ : Fully-developed fracture process zone length defined as  $\frac{EG_F}{f_t f_c}$ .
- $H$ ,  $S$  and  $B$ : Beam height, span and width.
- $\eta$ : Ratio between beam span and beam height  $\frac{S}{H}$ .
- $c$  and  $c^*$ : Reinforcement cover length and the normalized one  $c/H$ .
- $\beta$ : Brittleness number defined as  $\frac{H}{l_{fpz}}$ .

- $\beta_1$ : Brittleness number in the width direction defined as  $\frac{B}{l_{fpz}}$ .
- $y^*$ : Non-dimensional coordinate in the vertical direction  $\frac{y}{H} \in [0, 1]$ .
- $y_n$ : Location of the neutral fiber.
- $y_{gc}$ : Distance between the resulted compressive force and the neutral axis.
- $y_{ud}$ : Location of the cohesive crack tip.
- $y_{tip}$ : Location of the stress-free crack tip.
- $x^*$ : Non-dimensional coordinate in the horizontal direction  $\frac{x}{H} \in [0, \eta]$ .
- $\varphi(y^*)$ : The function that describes the crack trajectory.
- $\theta$ : The inclination angle of the shear reinforcement with respect to the x-direction.
- $\alpha$ : Local inclination angle (w.r.t. the x-axis) of the crack trajectory.
- $A_l$  and  $A_i$ : Area sum of the cross-section of the longitudinal and inclined rebars.
- $\rho_l$ : Longitudinal reinforcement ratio  $\frac{A_l}{BH}$ .
- $\rho_i$ : Incline/shear reinforcement ratio  $\frac{A_i}{BH}$ .
- $f_y^*$ : Steel yield strength normalized by concrete tensile strength  $\frac{f_y}{f_t}$ .
- $\sigma_c^*$ : Compressive stress normalized by concrete tensile strength  $\frac{\sigma_c}{f_t}$ .
- $\sigma_{lr}^*$ :  $f_y^* \rho_l$ .
- $\sigma_{ir}^*$ :  $0.75 f_y^* \rho_i \sin \theta$ .
- $M$  and  $M^*$ : Moment with respect to the fiber neutral,  $M^* = \frac{M}{f_t BH^2}$ .
- $M_i$ : Internal moment (calculated at a section).
- $M_c$  and  $M_t$ : Flexural moment generated by the compressive and the tensile tractions.

- $P$  and  $P^*$ : External load under a three-point-bend configuration,  $P^* = \frac{P}{f_t BH}$ .
- $Q(x)$  and  $Q^*(x^*)$ : Shear force at location  $x$ ,  $Q^*(x^*) = \frac{Q(x/H)}{f_t BH}$ .

## REFERENCES

- [1] Z.P. Bazant and J.K. Kim: Size effect in shear failure of longitudinally reinforced beams. *ACI Journal*, 81 (1984), 456–468.
- [2] F. J. Vecchio and M. P. Collins: The modified compression-field theory for reinforced concrete elements subjected to shear. *ACI Journal*, March-April (1986), 219–231.
- [3] J. G. Rots and R. De Borst: Analysis of mixed-mode fracture in concrete. *Journal of Engineering Mechanics*, 113 (1987), 1739–1758.
- [4] F. J. Vecchio and M. P. Collins: Predicting the response of reinforced concrete beams subjected to shear using modified compression field theory. *ACI Structural Journal*, (1988), 258–268.
- [5] P.J. Gustafsson and A. Hillerborg: Sensitivity in shear strength of longitudinal reinforced concrete beams to fracture energy of concrete. *ACI Structural Journal*, 85 (1988), 286–294.
- [6] Y.S. Jenq and S.P. Shah: Shear resistance of reinforced concrete beams - a fracture mechanics approach. *Fracture Mechanics: Application to concrete*, (1989), 237–258.
- [7] B.L. Karihaloo: Failure modes of longitudinally reinforced beams. *Application of Fracture Mechanics to Reinforced Concrete*, (1992), 523–546.
- [8] M. P. Collins, D. Mitchell, P. Adebar and F. J. Vecchio: A general shear design method. *ACI Structural Journal*, 93(1996), 36–60.

- [9] E. C. Bentz, F. J. Vecchio, and M. P. Collins: Simplified modified compression field theory for calculating shear strength of reinforced concrete elements. *ACI Structural Journal*, 103(2006), 614–624.
- [10] A. Hillerborg: Fracture mechanics concepts applied to moment capacity and rotational capacity of reinforced concrete beams. *Engineering Fracture Mechanics*, 35(1990), 233–240.
- [11] L. Biolzi: Mixed mode fracture in concrete beams. *Engineering Fracture Mechanics*, 35(1990), 187–193.
- [12] F. J. Vecchio: Analysis of shear-critical reinforced concrete beams. *ACI Structural Journal*, 97(2000).
- [13] G. Ruiz, M. Elices, and J. Planas: Experimental study of fracture of lightly reinforced concrete beams. *Materials and Structures*, 31(1998), 683–691.
- [14] P. Bocca, A. Carpinteri, and S. Valente: Mixed mode fracture of concrete. *International Journal of Solids and Structures*, 27 (1991), 1139–1153.
- [15] BS8110: Part I: Structural use of concrete: Code of practise for design and construction. *British Standard Institution*, 1997.
- [16] A. Carpinteri, J. R. Carmona, and G. Ventura: Failure mode transition in RC beams. Part 1: Theoretical model. *ACI Structural Journal*, 2011.
- [17] A. Carpinteri, J. R. Carmona, and G. Ventura: Failure mode transition in RC beams. Part 2: Experimental test. *ACI Structural Journal*, 2011.
- [18] Comité Euro International du Béton and Federation International de la Précontrainte: Model code for concrete structures. CEB-FIP International recommendations. 1993.
- [19] A. Hillerborg, M. Modeer, and P. E. Peterson: Analysis of crack formation and crack growth in concrete by means of fracture mechanics and finite element. *Cement and Concrete Research*, 6 (1976), 773–782.
- [20] British Standards Institution. Eurocode 2: Design of concrete structures part 1: General rules and rules for buildings. (1992).
- [21] M. T. Kazemi and V. Shahvari: Mixed mode fracture of concrete: An experimental investigation. *Scientia Iranica*, 11(2004), 378–385.
- [22] E. Montoya, F. J. Vecchio, and S. A. Sheikh: Compression field modeling of confined concrete: Constitutive models. *Journal of Materials in Civil Engineering*, 18(2006), 510–517.
- [23] A.R. C. Murthy, G. S. Palani, and N. R. Iyer: State-of-the-art review on fracture analysis of concrete structural components. *Sadhana*, 34(2009), 345–367.
- [24] A. Muttoni and M.F. Ruiz: Shear strength of members without transverse reinforcement as function of critical shear crack width. *ACI Structural Journal*, 105(2008), 163–172.
- [25] Y.N. Rabotnov: On the equation of state of creep. *Progress in Applied Mechanics*, (1963), 307.
- [26] C. Rosello and M. Elices: Fracture of model concrete 1. types of fracture and crack path. *Cement and Concrete Research*, 34 (2004), 1441–1450.
- [27] G. Ruiz, A. Pandolfi, and M. Ortiz: Three-dimensional cohesive modeling of dynamic mixed-mode fracture. *International Journal of Numerical Methods in Engineering*, 52 (2001), 97–120.

- [28] L. Saucedo, R.C. Yu, and G. Ruiz: Fully-developed FPZ length in quasi-brittle materials. *International Journal of Fracture*, accepted.
- [29] R.G Mathey, and D. Watsein: Shear strength of beams without web reinforcement containing deformed bars of different yield strengths. *ACI Journal*, 60(2),(1963),183207.
- [30] K.G. Moody, I.M. Viest, R.C Ester and E. Hognestad, E.:Shear strength of reinforcement concrete beams Part 1- Test simple beams. *ACI Journal*, 26(4)(1954), 317332.
- [31] J. M. Yang, K.H. Min, H.O. Shin, and Y. S. Yoon: The use of t-headed bars in high-strength concrete members. *FraMCoS-7*, 50 (2010), 1328–1335.
- [32] R. C. Yu, L. Saucedo, and G. Ruiz: Finite-element study of the diagonal-tension failure in reinforced concrete beams. *International Journal of Fracture*, 169 (2011), 169–182.